

Sensitivity of the electrocardiographic forward problem to the heart potential measurement noise and conductivity uncertainties

Rajae Aboulaich, Najib Fikal, El Mahdi Guarmah, Nejib Zemzemi

► To cite this version:

Rajae Aboulaich, Najib Fikal, El Mahdi Guarmah, Nejib Zemzemi. Sensitivity of the electrocardiographic forward problem to the heart potential measurement noise and conductivity uncertainties. Colloque africain sur la recherche en informatique et mathématiques appliquées, CARI 2016, Oct 2016, Hammamet, Tunisia. hal-01402938

HAL Id: hal-01402938

<https://hal.inria.fr/hal-01402938>

Submitted on 25 Nov 2016

HAL is a multi-disciplinary open access archive for the deposit and dissemination of scientific research documents, whether they are published or not. The documents may come from teaching and research institutions in France or abroad, or from public or private research centers.

L'archive ouverte pluridisciplinaire **HAL**, est destinée au dépôt et à la diffusion de documents scientifiques de niveau recherche, publiés ou non, émanant des établissements d'enseignement et de recherche français ou étrangers, des laboratoires publics ou privés.

1. Introduction

Many studies have been performed on the forward problem of electrocardiography, in order to create more accurate methods allowing to find the electrical potential on the heart surface. However the data required by the mathematical electrocardiographic model, is in practice subject to uncertainties due to measurement errors or modeling assumptions and the resulting lack of knowledge. Therefore the idea of uncertainties quantification has attracted much interest in the last few years [1, 4]. The goal is to propagate information on the uncertainty of input data to the solution of a PDE [5]. Moreover the electrical potential in the torso depends on some physical parameters and on the geometry of the patient. In this work we are interested in studying the effect of the conductivity uncertainties, and also epicardial boundary data, in the ECG forward problem solved via stochastic finite element method (SFEM). For this aim we consider a stochastic approach in which the parameters of the model will be viewed as having statistical distributions, then as result the solutions of the stochastic system obtained have statistical characteristics, and we can determine the mean and the standard deviation of the electrical potential in the torso.

2. Stochastic forward problem of electrocardiography

2.1. Function spaces and notation

We give in the following a short overview of the notations, and definition of the stochastic Sobolev space used throughout this paper. Let D be the spacial domain. Ω is sample space that belongs to a probability space (Ω, A, P) , A denotes the σ -algebra of subsets of Ω , and let P be the probability measure. Following the theory of Wiener [7], as well as Xiu and Karniadakis [5], we can represent any general second-order random process $X(\omega)$, $\omega \in \Omega$, in terms of a collection of finite number of random variables. We represent this random process by a vector $\xi = \xi(\omega) = (\xi_1(\omega), \dots, \xi_N(\omega)) \in \mathbb{R}^N$, where N is the dimension of the approximated stochastic space. We assume that each random variable is independent, its image space is given by $\theta_i \equiv \xi_i(\Omega) \subset \mathbb{R}$. Each random variable is characterised by a probability density function (PDF) $\rho_i : \theta_i \rightarrow \mathbb{R}^+$, for $i = 1, \dots, N$. Then, we define the joint PDF of the random vector ξ

$$\rho(\xi) = \prod_{i=1}^N \rho_i(\xi_i) \quad \forall \xi \in \theta,$$

where the support of ρ is $\theta = \prod_{i=1}^N \theta_i$. The probability measure on θ is $\rho(\xi)d\xi$. As commented in [5], this allows us to conduct numerical formulations in the finite dimensional (N-dimensional) random space θ .

In this paper we treat a stochastic problem of electrocardiography, and we suppose that the conductivity parameter and the epicardial boundary data two different are independent source of uncertainties two different and independent source of uncertainties, which will be represented by two random process. For the conductivity parameter random process we define the probability space (respectively the vector of random variables, PDF, the PDF support) with (Ω_0, A_0, P_0) , (respectively ξ_0, ρ_0, θ_0) and with (Ω_1, A_1, P_1) , (respectively ξ_1, ρ_1, θ_1) for the epicardial data random process.

Let us denote $\theta = \theta_0 \times \theta_1$ and $L^2(\theta) = L^2(\theta_0) \times L^2(\theta_1)$ the space of random variables X with finite second moments :

$$\mathbb{E}[X^2(\xi_0, \xi_1)] = \int_{\Theta_1} \left(\int_{\Theta_0} X^2(\xi_0, \xi_1) \rho(\xi_0) d\xi_0 \right) \rho(\xi_1) d\xi_1 < +\infty,$$

where $\mathbb{E}[\cdot]$ denotes the mathematical expectation operator. This space is a Hilbert space with respect to the inner product :

$$\langle X, Y \rangle_{L^2(\Theta)} = \mathbb{E}[XY] = \int_{\Theta_1} \left(\int_{\Theta_0} XY(\xi_0, \xi_1) \rho(\xi_0) d\xi_0 \right) \rho(\xi_1) d\xi_1$$

Additionally, we consider a spatial domain D and we define the tensor product Hilbert space $H^1(D) \otimes L^2(\Theta)$ of second-order random fields as :

$$L^2(D) \otimes L^2(\Theta) = \left\{ u : D \otimes \Theta \rightarrow \mathbb{R}, \int_{\Theta_1} \left(\int_{\Theta_0} \int_D |u(x, \xi_0, \xi_1)|^2 dx \rho(\xi_0) d\xi_0 \right) \rho(\xi_1) d\xi_1 \right\}$$

Analogously, the tensor product spaces $H^1(D) \otimes L^2(\Theta)$ and $H_0^1(D) \otimes L^2(\Theta)$ can be defined.

2.2. Stochastic formulation of the forward problem

Under our assumption the conductivity uncertainties and epicardial boundary data uncertainties do not interact, and they are supposed to be independent each other, consequently we represent the stochastic forward solution of the Laplace equation as random field depending to the both kinds of uncertainties. For the space domain we use a 2D computational mesh of the torso geometry (see Figure 1)

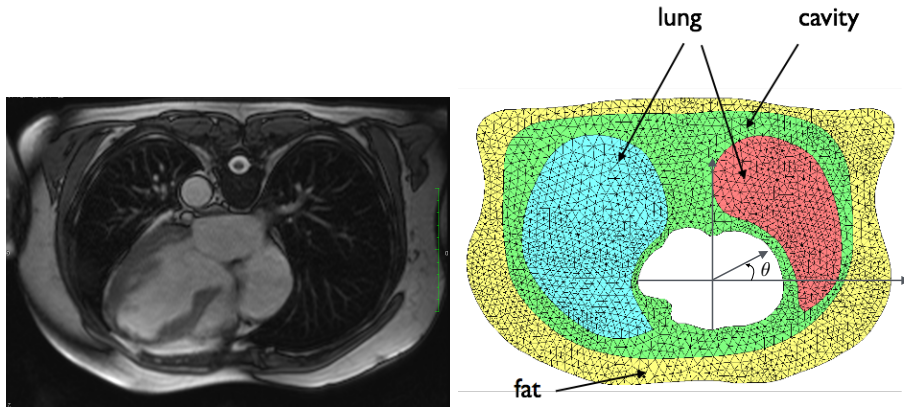


Figure 1 – MRI 2D slice of the torso (left), 2D computational mesh of the torso geometry showing the different regions of the torso considered in this study : fat, lungs and torso cavity, (right). The angle θ is the second polar coordinate.

Since we suppose that the conductivity parameter (σ) depends on the space (x) and on the stochastic variable (ξ_0), and the boundary epicardial data (f) depends on the space (x) and on a stochastic variable (ξ_1). Thus, the solution of the Laplace equation will depend on space and the both stochastic variables $u(x, \xi_0, \xi_1)$. The stochastic forward problem of electrocardiography can be written as follows

$$\begin{cases} \nabla \cdot (\sigma(x, \xi_0) \nabla u(x, \xi_0, \xi_1)) = 0 & \text{in } D \times \Omega, \\ u(x, \xi_0, \xi_1) = f(x, \xi_1) & \text{on } \Gamma_i \times \Omega, \\ \sigma(x, \xi_0) \frac{\partial u(x, \xi_0, \xi_1)}{\partial n} = 0 & \text{on } \Gamma_c \times \Omega, \end{cases} \quad (1)$$

Where, Γ_i and Γ_c are the epicardial and torso boundaries respectively.

The weak formulation of SPDEs is based on an extension of the deterministic theory [3], test function become random fields and an integration over stochastic space is done with respect to the corresponding measure. Thus, the weak form involves expectations of the weak problem formulation in the physical space. Then, denoting by u_f the extension of f to the whole domain, we look for $\tilde{u} \in H_0^1(D) \otimes L^2(\Theta)$, where $\tilde{u} = u - u_f$ is the weak solution of (1), if for all $v \in H_0^1(D) \otimes L^2(\Theta)$, we have :

$$\mathbb{E} \left[\int_D \sigma(x, \xi_1) \nabla \tilde{u}(x, \xi_0, \xi_1) \cdot \nabla v(x, \xi_0, \xi_1) dx \right] + \mathbb{E} \left[\int_D \sigma(x, \xi_1) \nabla u_f(x, \xi_0) \cdot \nabla v(x, \xi_0, \xi_1) dx \right] = 0. \quad (2)$$

3. Descretization of the stochastic forward problem

A stochastic process $X(\xi)$ of a parameter or a variable X is represented by weighted sum of orthogonal polynomials $\{\Psi_i(\xi)\}$ denoting the generalized chaos polynomial. More details about the different choices of PDFs could be found in [5].

We have

$$X(\xi) = \sum_{i=0}^p \hat{X}_i \Psi_i(\xi),$$

where \hat{X}_i are the projections of the random process on the stochastic basis $\{\Psi_i(\xi)\}_{i=1}^p$ with respect to the joint PDF ρ .

$$\hat{X}_i = \int_{\Omega} X(\xi) \Psi_i(\xi) d\rho = \langle X(\xi) \cdot \Psi_i(\xi) \rangle_{\rho}.$$

In order to solve the equation (2) we use the stochastic Galerkin (SG) method to compute the approximate solutions. To develop this method, we denote $Y_{\sigma}^p \subset L^2(\Theta_{\theta})$ and $Y_{u_f}^p \subset L^2(\Theta_1)$ the stochastic approximation spaces, and we have $Y_{\sigma}^p \times Y_{u_f}^q \subset L^2(\Theta)$. In our case we suppose that the conductivity parameter varie uniformly like in [4, 2] and we use the Legendre chaos polynomials which are more suitable for uniform probability density, in other hand we assigned Gaussian probability density to the epicardial boundary data, the corresponding stochastic orthogonal basis to Gaussian random field is Hermite chaos polynomials [5].

$$Y_{\sigma}^p = \text{span} \{ L_0, \dots, L_p \}.$$

$$Y_{u_f}^p = \text{span} \{ H_0, \dots, H_p \}.$$

In this study we have targeted to evaluate in the same time, two different source of uncertainties on the electrical potential, then σ , u_f and u are now expressed in the Galerkin space $Y_{\sigma}^p \times Y_{u_f}^q$ as follows :

$$\sigma(x, \xi_0) = \sum_{l=1}^r \hat{\sigma}_l(x) L_l(\xi_0). \quad (3)$$

$$u_f(x, \xi_1) = \sum_{k=1}^q (\tilde{u}_f)_k(x) H_k(\xi_1). \quad (4)$$

$$u(x, \xi_0, \xi_1) = \sum_{i=1}^p \sum_{j=1}^q \hat{u}_{ij}(x) L_i(\xi_0) H_j(\xi_1) \quad (5)$$

By substituting (4),(3),(5) into the stochastic diffusion equation (1) and by projecting the result on the polynomial basis $\{L_m(\xi_0)H_n(\xi_1)\}_{m,n=1}^{(p,q)}$:

For $m = 1, \dots, q$ et $n = 1, \dots, p$,

$$\begin{aligned} \sum_{i=1}^p \sum_{j=1}^q \sum_{l=1}^r D_{jn} C_{iml} \nabla \cdot (\hat{\sigma}_l(x) \nabla \hat{u}_{ij}(x)) &= 0 && \text{in } D, \\ \hat{u}_{11}(x) &= (\tilde{u}_f)_1(x) && \text{on } \Gamma_i, \forall i = 1, \dots, p, \\ \hat{u}_{12}(x) &= (\tilde{u}_f)_2(x) && \text{on } \Gamma_i \forall i = 1, \dots, p, \\ \hat{u}_{ij}(x) &= 0 && \text{on } \Gamma_i \forall i = 2, \dots, p, j = 3, \dots, q, \\ \hat{\sigma}_l(x) \frac{\partial \hat{u}_{ij}(x)}{\partial n} &= 0 && \text{on } \Gamma_c \forall i = 1, \dots, p, j = 1, \dots, q, \end{aligned} \quad (6)$$

Where $C_{iml} = \mathbb{E}[L_i(\xi_0), L_m(\xi_0), L_l(\xi_0)]$ et $D_{jn} = \mathbb{E}[H_j(\xi_1), H_n(\xi_1)]$.

For the spatial domain, we define a subspace $V_h \subset H_0^1(D)$ of standard Lagrange finite element functions on a triangulation of the domain D .

$$V_h := \text{span} \{\phi_1, \phi_2, \dots, \phi_{N_x}\}$$

Obviously this ordering induces the following block structure of the linear system of equations :

$$\begin{bmatrix} A^{(1,1;1,1)} & A^{(1,1;1,2)} & \dots & A^{(1,1;1,q)} & A^{(1,1;2,1)} & \dots & A^{(1,1;p,q)} \\ A^{(1,2;1,1)} & A^{(1,2;1,2)} & \dots & A^{(1,2;1,q)} & A^{(1,2;2,1)} & \dots & A^{(1,2;p,q)} \\ \vdots & \vdots & \dots & \vdots & \vdots & \dots & \vdots \\ A^{(1,q;1,1)} & A^{(1,q;1,2)} & \dots & A^{(1,q;1,q)} & A^{(1,q;2,1)} & \dots & A^{(1,q;p,q)} \\ A^{(2,1;1,1)} & A^{(2,1;1,2)} & \dots & A^{(2,1;1,q)} & A^{(2,1;2,1)} & \dots & A^{(2,1;p,q)} \\ \vdots & \vdots & \dots & \vdots & \vdots & \dots & \vdots \\ A^{(p,q;1,1)} & A^{(p,q;1,2)} & \dots & A^{(p,q;1,q)} & A^{(p,q;2,1)} & \dots & A^{(p,q;p,q)} \end{bmatrix} \begin{bmatrix} \hat{U}_{11} \\ \hat{U}_{12} \\ \vdots \\ \hat{U}_{1q} \\ \hat{U}_{21} \\ \vdots \\ \hat{U}_{pq} \end{bmatrix} = \begin{bmatrix} B^{11} \\ B^{12} \\ \vdots \\ B^{1q} \\ B^{21} \\ \vdots \\ B^{pq} \end{bmatrix}$$

where every matrix $A^{(i,j;m,n)} \in \mathbb{R}^{N_x} \times \mathbb{R}^{N_x}$ is a linear combination of finite element stiffness matrices

$$A^{(i,j;m,n)} = D_{j,n} \sum_{l=1}^r C_{iml} K_l \quad \forall i, m = 1, \dots, p; j, n = 1, \dots, q, \quad (7)$$

$$K_l = [K_l]_{h,t} = (\sigma_l \nabla \phi_h \cdot \nabla \phi_t) \quad \forall l = 1, \dots, r, \quad (8)$$

h denotes the degrees of freedom of the nodes of the mesh in which the electrical potential values is unknown.

Similarly, every vector $B^{ij} \in \mathbb{R}^{N_x}$ is a linear combination of finite element load vectors :

$$B^{ij} = \sum_{l=1}^r C_{iml} f_l \quad \forall i = 1, \dots, p, j = 1, \dots, q, \quad (9)$$

$$f_l = \sum_{x_h \in \Gamma_i} \hat{u}_{ij} (\sigma_l \nabla \phi_h \cdot \nabla \phi_t) \quad \forall l = 1, \dots, r, \quad (10)$$

with h denoting the degrees of freedom of the (known) Dirichlet boundary conditions of the solution.

4. Results

In this section we conduct the numerical simulation obtained in order to show the influence of the conductivity variabilities and the epicardial potential data uncertainties on the electrical potential in the torso. For instance we suppose that the electrical potential in the heart boundary is equal to U_{ex} .

$$U_{ex} = \sin(y).$$

Since we assume that the uncertainty of the conductivity value follows a uniform probability density, as probability density functions ρ_0 we use the Legendre polynomials defined on the interval $\Omega = [-1, 1]$. We also suppose that the true conductivity uncertainty interval is centered by σ_T , the true conductivity see Table 1. In other hand U_{ex} will represent the mean of the Gaussian random field representing the epicardial boundary data uncertainty, we denote its stdev by (ν) .

organ category	conductivity (σ_T :S/m)
lungs	0.096
torso cavity	0.200
fat	0.045

Tableau 1 – Conductivity values corresponding to the organs that are considered in the model.

In the following we present four cases, in the first case we only study the effect of epicardial boundary data uncertainties where we gradually increase the stdev ν from zero to 50%. In the second (respectively, third, fourth) case we add the effect of fat (respectively, cavity, lung) with $\pm 50\%$ of uncertainties. Figure 2 summarize the obtained results for all cases. First we see that the forward solution after adding epicardial boundary data uncertainties is more sensitive to the torso cavity and lung conductivities than it is for fat. This result is in line with the numerical results obtained in [4, 2]. Second we remark that the influence of organs conductivity uncertainties disappear when $\nu \geq 10^{-1}$ and all curves take the same values as the case with only epicardial boundary data uncertainty. Figure 3 displays an example for obtained results with respect to lung with $\pm 50\%$ of conductivity uncertainties and epicardial boundary data uncertainty with different values of ν . Figure 3(a) shows the mean value of $u(x, \xi_0, \xi_1)$. Figure3 (b) (respectively Figure 3(c), Figure3(d), and Figure3(e)) shows $u(x, \xi_0, \xi_1)$ stdev with respect to $\pm 50\%$ lung uncertainties and $\nu = 0.03$ (respectively $\nu = 0.05, \nu = 0.1, \nu = 0.5$), finally Figure3(f) represents the case supposing that there is no conductivity uncertainties.

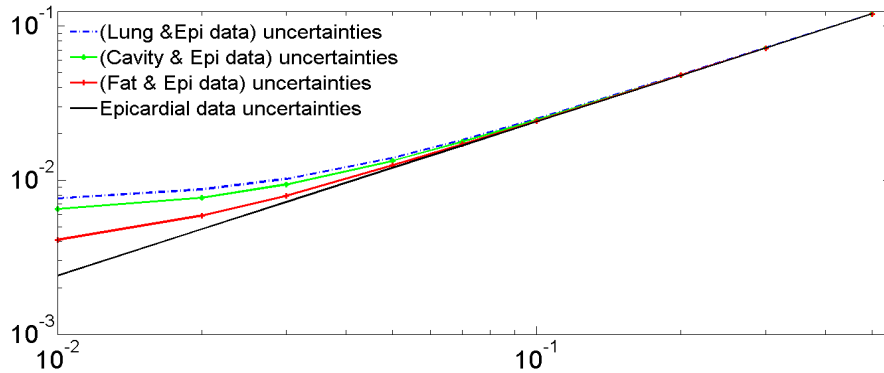


Figure 2 – The effects of $\pm 50\%$ uncertainty to each organ conductivity from its reference conductivity, and different levels of uncertainty on the the epicardial boundary data. X-axis denote the different stdev value (ν) of the Gaussian epicardial data boundary field. Y-axis the mean square of the stdev value of $u(x, \xi_0, \xi_1)$.

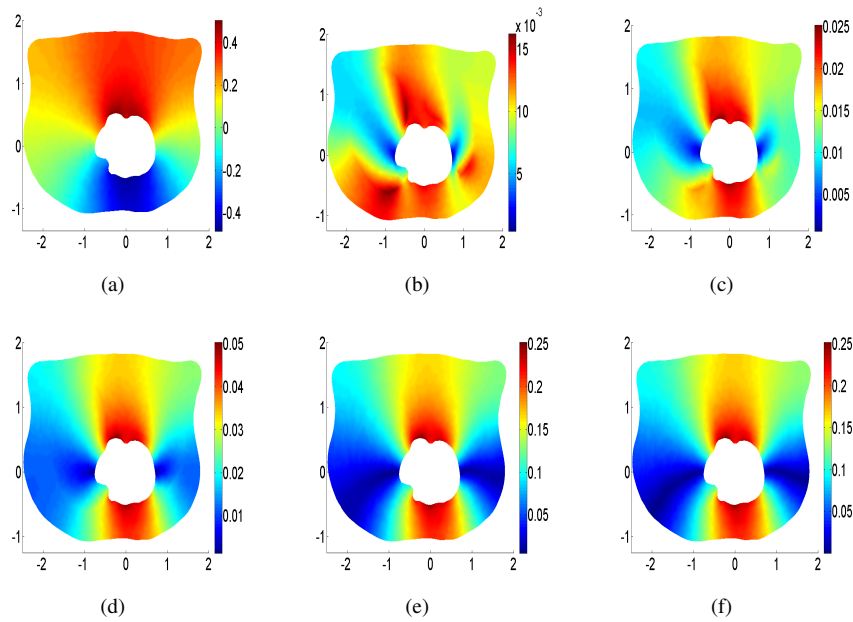


Figure 3 – Mean value of the SFE panel (a). Standard deviation of the SFE solution for $\pm 50\%$ of uncertainty for lung and epicardial data uncertainty for $\nu = 0.03$ panel(b) (respectively $\nu = 0.05$ panel(c), $\nu = 0.1$ panel(d), $\nu = 0.5$ panel(e)). Panel(f) shows the Standard deviation of the SFE solution with only epicardial data uncertainty for $\nu = 0.5$

5. Conclusion :

This work is a novel approach studying the sensitivity of forward problem of electrocardiography, with respect to different sources of uncertainty using chaos polynomial and SFE method. The obtained results allow to classify the influence of each parameter. We conclude that epicardial potential boundary data uncertainty have a strong effect on forward problem solution errors, compared to the organs conductivity, which at some level of boundary data uncertainty becomes insignificant. This finding suggests that the precise determination of the epicardial boundary data is very important. In a next work we will solve the inverse problem following the formulation presented in [1], using stochastic approach developed in this work, and we will study the uncertainties in the case of the inverse problem.

Références

- [1] A. OOSTEROM, G.J. HUISKAMP, « The effect of torso inhomogeneities on body surface potentials quantified using "tailored" geometry », *Journal of electrocardiology*, vol. 22, n° 1, 1989.
- [1] R. ABOULAICH, A. BEN ABDA, M. KALLEL, « missing boundary data reconstruction via an approximate optimal control », *Inverse Problems and Imaging*, vol. 2, n° 4, 2008.
- [2] R. ABOULAICH, N. FIKAL, E. EL GUARMAH, N. ZEMZEMI, « Stochastic Finite Element Method for torso conductivity uncertainties quantification in electrocardiography inverse problem », *Accepted in Math. Model. Nat. Phenom.*, vol. Jan. (2016).
- [3] I. BABUSKA, R. TEMPONE, G.E. ZOURARIS, « Galerkin finite element approximations of stochastic elliptic partial differential equations », *SIAM Journal on Numerical Analysis*, vol. 42, n° 2, 2005.
- [4] S.E. GENESER, R.M. KIRBY, R.S. MACLEOD, R.M. KIRBY, « Application of stochastic finite element methods to study the sensitivity of ECG forward modeling to organ conductivity », *Biomedical Engineering, IEEE Transactions*, vol. 55, n° 1, 2008.
- [5] D. XIU, G.E. KARNIADAKIS, « Modeling uncertainty in flow simulations via generalized polynomial chaos », *Elsevier, J.Comput.Phys.*, vol. 194, 2003.
- [7] S. WIENER, « The homogeneous chaos », *Am. J. Math.*, vol. 60, 1998.